BISPECTRUM MODULATION FOR JAMMING REJECTION ON SATELLITE COMMUNICATION CHANNELS

Final Technical Report
12 May 1995

Advanced Research Projects Agency (ARPA)
Defense Small Business Innovation Research Program
ARPA Order No. 5916, Amdt
Issued by U.S. Army Missile Command Under
Contract No. DAAH01-94-C-R256
CDRL No. A002

Prepared by:
Dr. Richard J. Barton, Principal Investigator, Project
Neoteric Technologies, Inc.
1326 Suncrest Drive
Cincinnati, OH 45208
(513) 321-6701

Contract Expiration Date: 30 April 1995

The views and conclusions contained in this document are those of the authors and should not be interpreted as representing the official policies, either expressed or implied, of the Advanced Research Projects Agency or the U.S. Government.

1. Introduction

The Global Grid communications environment is designed to provide a high-data-rate network that supports the full complement of DoD communications needs. Satellite links are an integral part of the Global Grid concept which extends the connectivity to individual mobile units and jointly operating forces at isolated locations. However, satellite channels are vulnerable to jamming, in particular when a high data rate is required. To overcome the jamming problem, the traditional approach is to design modulation techniques such that, on the average, the spectrum of the signal looks like the spectrum of a white noise process. This together with channel coding provides immunity against jamming. The main problem with this approach is that it requires a much larger spectrum than that of the data sequence; hence, the available spectrum on the link is used mostly for jamming protection and not for data communications.

The traditional modulation techniques employed on satellite communication links are based on various properties of the second-order spectrum of the modulation wave form. In this study we have explored the utility and performance of a new family of modulation schemes that exploit the properties of the higher-order *cumulant sequences* and associated *polyspectra* of the waveform. In particular, we have investigated an approach in which the third-order polyspectrum, which is generally referred to as the bispectrum, is modulated. To determine the performance characteristics of this bispectral modulation scheme, we have considered two different detector structures, for which we have completed both theoretical and simulated performance analyses. We have studied the performance of each detector structure in both an additive white Gaussian noise environment and a partial-band jamming environment, and we have demonstrated that bispectral modulation techniques can significantly outperform traditional anti-jamming modulation schemes, such as frequency-hopped, binary frequency-shift keying, in the presence of partial-band jamming. Our results also indicate that, even on an additive white Gaussian noise channel, bispectral modulation can be used in parallel with conventional noncoherent modulation techniques to increase the data rate on the channel or to reduce the sensitivity to synchronization errors between the transmitter and receiver.

This report is organized as follow. In Section 2, we present a brief introduction to polyspectra and one particular polyspectrum estimation technique. In Section 3, we discuss in detail the proposed modulation scheme and a simple technique for implementing it. The results of our performance analyses are presented in Sections 4 and 5, and in Section 6 we present some conclusions about the research and suggestions for further study. Considerably more detail regarding the advantages and direction of future research will be presented in our Phase II proposal, which will be submitted within 30 days.

2. Background and Definitions

In this section, we give some necessary background information on the properties of higher-order moments and polyspectra and a brief discussion of the polyspectrum estimation technique employed in this study.

Let $\{x(n)\}$ be a strictly stationary real random process. We assume, without loss of generality, that $\{x(n)\}$ has mean zero. The kth-order *cumulant sequence* for such a process is defined in terms of the first k moments of the process. For example, the second-, third-, and fourth-order cumulant sequences are given by:

$$C_2(n_1) = \mathrm{E}\{x(k)x(k+n_1)\},$$

$$C_3(n_1, n_2) = \mathrm{E}\{x(k)x(k+n_1)x(k+n_2)\},$$

$$C_4(n_1, n_2, n_3) = \mathrm{E}\{x(k)x(k+n_1)x(k+n_2)x(k+n_3)\} - \mathrm{E}\{x(k)x(k+n_1)\}\mathrm{E}\{x(k+n_2)x(k+n_3)\}$$
$$-\mathrm{E}\{x(k)x(k+n_2)\}\mathrm{E}\{x(k+n_1)x(k+n_3)\} - \mathrm{E}\{x(k)x(k+n_3)\}\mathrm{E}\{x(k+n_1)x(k+n_2)\},$$

where the symbol "E" represents the expectation operator, and k, n_1, n_2, and n_3 are arbitrary integers. Clearly $\{C_2(n_1)\}$ is just the covariance sequence of the process and $\{C_3(n_1,n_2)\}$ is the third moment sequence.

The kth-order *polyspectrum* of the process $S_k(\underline{\omega})$ is the multidimensional Fourier transform of the corresponding cumulant sequence; that is,

$$S_k(\underline{\omega}) = S_k(\omega_1, \cdots, \omega_{k-1}) = \sum_{n_1=-\infty}^{\infty} \cdots \sum_{n_{k-1}=-\infty}^{\infty} C_k(n_1, \cdots, n_{k-1}) e^{-i(\omega_1 n_1 + \cdots + \omega_{k-1} n_{k-1})}$$

For $k = 2$, the polyspectrum is clearly just the power spectrum of the process. For $k = 3$ and $k = 4$ (the other two cases of most practical interest), the polyspectra are usually referred to as the *bispectrum* and *trispectrum*, respectively. Due to the symmetries and periodicities of the polyspectrum, it is completely defined by its values on a nonunique *principal domain* $D_k \subset R^{k-1}$. For example, the principal domain of the bispectrum is generally taken to be:

$$D_3 = \{(\omega_1, \omega_2): 0 \le \omega_1 \lesseqgtr \pi,\ 0 \le \omega_2 \le \min(\omega_1, 2\pi - 2\omega_1)\}.$$

This region is depicted in Figure 1.

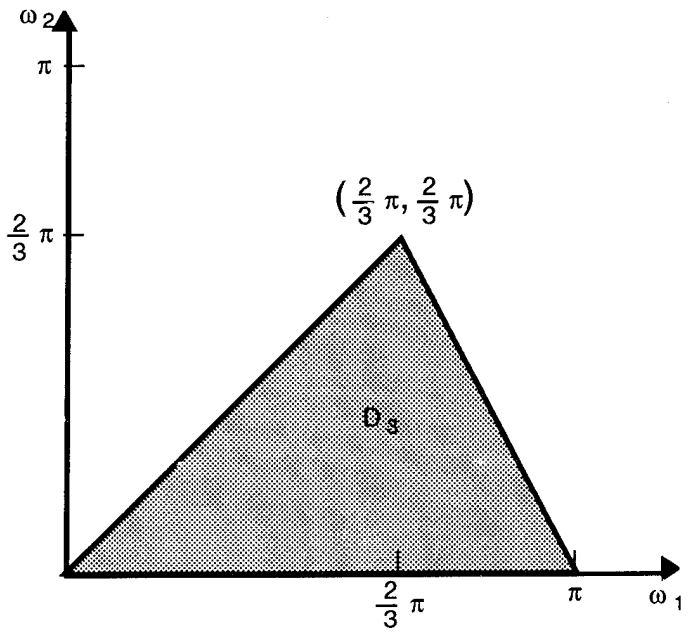

Figure 1. Principal Domain of the Bispectrum

Polyspectra have many interesting properties, but the following three are perhaps the most useful:

1. If $\{x(n)\}$ and $\{y(n)\}$ are independent processes with polyspectra S_k^x and S_k^y, then $S_k^{x+y} = S_k^x + S_k^y$.
2. If $\{x(n)\}$ is a Gaussian process, then $S_k^x \equiv 0$ for $k > 2$.
3. If $\{y(n)\}$ is produced as the output of a linear system with frequency response $H(\omega)$ driven by a process $\{x(n)\}$, then

$$S_k^y(\underline{\omega}) = H(\omega_1)H(\omega_2)\cdots H(\omega_{k-1})H(-\omega_1-\omega_2-\cdots-\omega_{k-1})S_k^x(\underline{\omega}).$$

In this report, we will be concerned exclusively with the bispectrum, which we will denote simply as $B(\omega_1,\omega_2)$. The following examples provide some simple illustrations of the bispectrum and its properties.

Example 1 - Linear processes. If $\{\varepsilon(n)\}$ is an *i.i.d.* sequence of random variables such that

$$\mu_3^\varepsilon = E\left\{\varepsilon(n)^3\right\} \neq 0,$$

then $B_\varepsilon(\omega_1,\omega_2) \equiv \mu_3^\varepsilon$. In general, if $\{x(k)\}$ has the linear representation

$$x(k) = \sum_{n=-\infty}^{\infty} h(n)\varepsilon(k-n),$$

then

$$B_x(\omega_1,\omega_2) = \mu_3^{\varepsilon} H(\omega_1)H(\omega_2)H(-\omega_1-\omega_2),$$

where

$$H(\omega) = \sum_{n=-\infty}^{\infty} h(n)e^{-i\omega n}$$

Example 2 - Sum of independent sinusoids. If ϕ is a random phase, uniformly distributed on $[0,2\pi]$, then the bispectrum of the process $\{\cos(k\lambda+\phi)\}$ is identically zero for any radian frequency λ. In general, if

$$x(k) = \sum_{n=0}^{N-1} \cos\left(k\lambda_n + \phi_n\right),$$

where $\{\lambda_n\}$ is a given set of frequencies and $\{\phi_n\}$ is a collection of *i.i.d.* random variables uniformly distributed on $[0,2\pi]$, then $B_x(\omega_1,\omega_2) \equiv 0$.

Example 3 - Phase Coupling. Consider the process

$$x(k) = \cos\left(k\lambda_1 + \phi_1\right) + \cos\left(k\lambda_2 + \phi_2\right) + \cos\left(k\lambda_3 + \phi_3\right),$$

where

$$\lambda_2 < \lambda_1,\ \lambda_3 = \lambda_1 + \lambda_2,\ \ \phi_3 = \phi_1 + \phi_2,$$

and ϕ_1 and ϕ_2 are *i.i.d.* random variables uniformly distributed on $[0,2\pi]$. In this case, the third-order cumulant sequence is given by:

$$C_3^x(m,n) = \frac{1}{4}\left\{\cos(\lambda_1 n + \lambda_2 m) + \cos\left((\lambda_1+\lambda_2)n - \lambda_2 m\right) + \cos\left((\lambda_1+\lambda_2)n - \lambda_1 m\right)\right\}$$

$$+\frac{1}{4}\left\{\cos(\lambda_1 m + \lambda_2 n) + \cos\left((\lambda_1+\lambda_2)m - \lambda_2 n\right) + \cos\left((\lambda_1+\lambda_2)m - \lambda_1 n\right)\right\}.$$

Consequently, the bispectrum of the process evaluated in D_3 shows an impulse at the point (λ_1,λ_2). This is in sharp contrast to the previous example in which the phases were not coupled and the bispectrum was identically zero. It is for this reason that the bispectrum has been proposed as an efficient means of detecting quadratic phase coupling in a process [1].

Example 4 - Bicoherence. Let $\{x(n)\}$ be an arbitrary process, and consider the quantity:

$$\beta_x(\omega_1,\omega_2) = \frac{B_x(\omega_1,\omega_2)}{\sqrt{S_2^x(\omega_1)S_2^x(\omega_2)S_2^x(\omega_1+\omega_2)}}.$$

This quantity, which we will refer to as the *bicoherence* of the process, represents a normalized, scale invariant version of the bispectrum analogous to the more familiar spectral coherence function. Unlike the spectral coherence, the magnitude of the bicoherence of a process is not necessarily bounded; however, it can be shown that the variance of a conventional estimate of the bicoherence is essentially independent of the power of the process . Furthermore, it follows immediately from Property 3 above that the magnitude of the bicoherence is invariant under all linear transformations, and the phase is invariant under linear transformations with linear phase

response. That is, if $\{y(n)\}$ is the output of a linear system with frequency response

$$H(\omega) = |H(\omega)| e^{i\arg(H(\omega))}$$

driven by the process $\{x(n)\}$, then

$$|\beta_y(\omega_1, \omega_2)| = |\beta_x(\omega_1, \omega_2)|,$$

and if $\arg(H(\omega)) = \kappa \cdot \omega$, where κ is an arbitrary constant independent of ω, then

$$\arg(\beta_y(\omega_1, \omega_2)) = \arg(\beta_x(\omega_1, \omega_2)).$$

For communication purposes, this is a very intriguing property of the bispectrum (or any of the higher-order polyspectra) since it implies that a communication scheme based on amplitude modulation of the bicoherence will be insensitive to any linear distortions introduced by the communication channel. Similarly, a communication scheme based on phase modulation of the bicoherence will be insensitive to distortions with linear phase response.

A Class of Polyspectrum Estimates

One of the most popular conventional polyspectrum estimation techniques was introduced by Brillinger and Rosenblatt in [2]. To define the Brillinger-Rosenblatt (B-R) estimate, let $\{x_N(n)\}$ be a data sample of length N with discrete Fourier transform $\{X_N(m)\}$, and let W be a continuous, $(k\text{-}1)$-dimensional frequency-domain averaging function that satisfies

$$\text{(i)}\ W(\underline{\omega}) \geq 0,$$

$$\text{(ii)}\ W(-\underline{\omega}) = W(\underline{\omega}),$$

$$\text{(iii)}\ \int_{R^{k-1}} W(\underline{\omega}) d\underline{\omega} = 1.$$

For any $0 < c < 1$, define the scaled version of W by $W_N(\underline{\omega}) = N^{(1-c)(k-1)} W\left(N^{1-c}\underline{\omega}\right)$. Define the generalized periodogram by:

$$I_N^x(n_1, \cdots, n_{k-1}) = \frac{1}{N} X_N(n_1) X_N(n_2) \cdots X_N(n_{k-1}) X_N(-n_1 - n_2 - \cdots - n_{k-1}),$$

and let the indicator function χ be defined by:

$$\chi(\underline{\omega}) = \begin{cases} 0 & \text{if } \sum_{j \in J} \omega_j \equiv 0 \pmod{2\pi} \text{ for any } J \subset \{1, \cdots, k-1\}, \\ 1 & \text{otherwise.} \end{cases}$$

Using the above notation, the B-R estimate of the true polyspectrum $S_k^x(\underline{\omega})$ at an arbitrary point is given by:

$$\hat{S}_k^x(N, W, \underline{\omega}) = \left(\frac{2\pi}{N}\right)^{k-1} \sum_{n_1=-\infty}^{\infty} \cdots \sum_{n_{k-1}=-\infty}^{\infty} W_N\left(\frac{2\pi n_1}{N} - \omega_1, \cdots, \frac{2\pi n_{k-1}}{N} - \omega_{k-1}\right)$$

$$\cdot \chi\left(\frac{2\pi n_1}{N}, \cdots, \frac{2\pi n_{k-1}}{N}\right) I_N^x(n_1, \cdots, n_{k-1}).$$

In particular, for this study, we always used an averaging parameter value of $c = 0.5$ and separable, two-dimensional rectangular averaging windows of the form:

$$W(\omega_1,\omega_2)=W_1(\omega_1)W_1(\omega_2),$$

$$W_1(\omega)=\begin{cases}\dfrac{1}{2\pi} & \text{if } |\omega|\le\pi,\\ 0 & \text{otherwise.}\end{cases}$$

Hence, all of our bispectrum estimates took the particular form:

$$\hat{B}_N(\omega_1,\omega_2)=\frac{1}{N^2}\sum_{n=1}^{N-1}\sum_{m=1}^{N-1}W_1\left(\frac{2\pi n}{N^{1/2}}-N^{1/2}\omega_1\right)W_1\left(\frac{2\pi m}{N^{1/2}}-N^{1/2}\omega_2\right)$$
$$\cdot X_N(n)X_N(m)X_N(n+m).$$

Similarly, all of our bicoherence estimates took the form:

$$\hat{\beta}_N(\omega_1,\omega_2)=\frac{\hat{B}_N(\omega_1,\omega_2)}{\hat{Z}_N(\omega_1,\omega_2)},$$

where

$$\hat{Z}_N(\omega_1,\omega_2)=\frac{1}{N^{5/2}}\sum_{n=1}^{N-1}\sum_{m=1}^{N-1}W_1\left(\frac{2\pi n}{N^{1/2}}-N^{1/2}\omega_1\right)W_1\left(\frac{2\pi m}{N^{1/2}}-N^{1/2}\omega_2\right)$$
$$\cdot|X_N(n)X_N(m)X_N(n+m)|.$$

The B-R estimation technique was employed primarily because the statistical behavior of such estimates is well understood. Furthermore, the B-R estimates can be computed very efficiently with a fast algorithm designed and implemented by the principal investigator [3].

3. Signal Design

There are many possible signal designs that one might use in order to encode information in the bispectrum or bicoherence of the transmitted waveform. In essence, each possible approach can be regarded as a generalization of a more conventional modulation technique, in which the higher-order moment (HOM) content of the signal is available in addition to the information transmitted in the conventional modulation. In situations where the channel performs approximately as an additive white Gaussian noise (AWGN) channel, the conventional detection scheme is often nearly optimal and will outperform detectors that attempt to exploit the HOM content of the signal. On the other hand, in situations where the principal source of channel degradation is something other than AWGN, such as fading or narrowband interference, considerable performance improvement can be realized by employing a detector that is designed to exploit the higher-order structure of the signal.

In this study, we considered baseband signals of the following form:

$$x(t)=m(t)\cdot\sum_{i=1}^{3}\cos\left(2\pi\lambda_{i-(-1)^p}\cdot t+\phi_{i-(-1)^p}\right),$$

Where $\{\lambda_i\}_{i=1}^{6}$ is a set of frequency elements, $\{\phi_i\}_{i=1}^{6}$ a set of phase elements, b the transmitted bit value (0 or 1), and $m(t)$ a *spreading signal*, which will be discussed in detail below. We will also assume the following relationships among the various elements:

$$\phi_{1-(-1)^b} \;\&\; \phi_{2-(-1)^b} \text{ uniformly distributed on } [2,\pi],$$

$$\lambda_{3-(-1)^b} = \lambda_{1-(-1)^b} + \lambda_{2-(-1)^b}, \text{ and}$$

$$\phi_{3-(-1)^b} = \phi_{1-(-1)^b} + \phi_{2-(-1)^b}.$$

Notice that such a signal is really a generalization of both a frequency-shift-keying (FSK) waveform, in which three phase-coupled frequency components are used to transmit each bit instead of a single component, and a direct-sequence spread-spectrum (DSSS) waveform, in which the spreading sequence is modulated onto a multiple-component carrier. Similarly, if the set $\{\lambda_i\}$ is allowed to vary randomly, the signal becomes a generalization of a frequency-hopped spread-spectrum (FHSS) waveform. For expository purposes, we will generally assume that the frequencies are fixed, but it should be remembered that this need not necessarily be the case.

We will be concerned primarily with the sampled version of this signal, denoted by the sequence $\{x^N(n)\}_{n=0}^{N-1}$, where

$$\begin{aligned} x^N(n) &= x(nT) \\ &= m(nT) \cdot \sum_{i=1}^{3} \cos\left(2\pi\lambda_{i-(-1)^b} \cdot nT + \phi_{i-(-1)^b}\right) \\ &\triangleq m^N(n) \cdot \sum_{i=1}^{3} \cos\left(\lambda^N_{i-(-1)^b} \cdot n + \phi_{i-(-1)^b}\right). \end{aligned}$$

Here, T is the sampling interval, and NT is the length of the bit interval. Notice that we have implicitly defined the *spreading sequence* $\{m^N(n)\}_{n=0}^{N-1}$, and the set of *normalized frequencies* $\{\lambda^N_{i-(-1)^b}\}_{i=1}^{3}$ using the relationships:

$$m^N(n) = m(nT),$$

$$\lambda^N = 2\pi T\lambda.$$

Since we will almost always be referring to the digital sequence rather than the analog signal, we will usually abuse notation somewhat and neglect to use the superscript "N" characters except when necessary to avoid confusion. Also, we will generally assume that a bit value of $b = 0$ is transmitted.

The main purpose of the spreading sequence $\{m(n)\}$ is to increase the bispectral bandwidth of the signal in order to improve the efficiency of the bispectrum estimates employed in the detector. As discussed above, the phase-coupled carrier itself has a bispectrum that takes the form of an impulse at a single point in the principal domain. This turns out to be problematic from a statistical standpoint, at least when using B-R estimates of the bispectrum and bicoherence, as we have done. This problem can be alleviated by modulating the carrier with a pseudo-random sequence having nonzero bispectrum and bandwidth chosen to match the "bandwidth" of the bispectrum estimator. In particular, if the bispectrum estimates are computed using an averaging parameter with value

$0 < c < 1$, then the bandwidth of the spreading sequence in the digital frequency domain should be of order N^{c-1} radians, where N is again the number of samples in a bit interval. This can be accomplished in the following manner.

Let $\{h(k)\}$ be the impulse response of a real-valued, low-pass linear filter with frequency response $H(\omega)$ and $\sum_{k=-\infty}^{\infty} h^2(k) = 1$, and let $\{h_N(k)\}$ be the scaled version of the impulse response with associated frequency response:

$$H_N(\omega) = N^{\frac{1-c}{2}} H\left(N^{1-c}\omega\right), \quad -\pi \le \omega \le \pi.$$

Let $\{u(k)\}$ be a zero-mean, *i.i.d.* random process with variance σ_s^2, third-order moment $m_3 \neq 0$, and bicoherence $\beta = m_3/\sigma_s^3$. Filter $\{u(k)\}$ with $\{h_N(k)\}$ to produce the spreading sequence $\{m(n)\}$, which will have spectrum, bispectrum, and bicoherence that satisfy:

$$S_m(\omega) = \sigma_s^2 \left|H_N(\omega)\right|^2,$$

$$B_m(\omega_1, \omega_2) = \mu_3 H_N(\omega_1) H_N(\omega_2) H_N(-\omega_1 - \omega_2),$$

$$\left|\beta_m(\omega_1, \omega_2)\right| = \begin{cases} \dfrac{\mu_3}{\sigma_s^3} & \text{if } B_m(\omega_1, \omega_2) \neq 0, \\ 0 & \text{otherwise.} \end{cases}$$

If $\{m(n)\}$ is generated in this fashion, then the transmitted signal $\{x(n)\}$ has spectrum, bispectrum, and bicoherence that satisfy (assuming $b = 0$):

$$S_x(\omega) = \frac{\sigma_s^2}{4} \sum_{i=1}^{3} \left\{\left|H_N(\omega - \lambda_i)\right|^2 + \left|H_N(\omega + \lambda_i)\right|^2\right\},$$

$$B_x(\omega_1, \omega_2) = \frac{\mu_3}{8} H_N(\omega_1 - \lambda_1) H_N(\omega_2 - \lambda_2) H_N(-\omega_1 - \omega_2 + \lambda_3), \text{ near } (\lambda_1, \lambda_2),$$

$$\left|\beta_x(\omega_1, \omega_2)\right| = \frac{\mu_3}{\sigma_s^3}, \text{ near } (\lambda_1, \lambda_2).$$

Now, in general, the bicoherence of the signal, when considered as a stationary random process, can be made arbitrarily large by choosing an *i.i.d.* sequence $\{u(k)\}$ with arbitrarily large skewness (i.e., the quantity m_3/σ_s^3) as the input to the filter $\{h_N(k)\}$. However, in practice, the bispectrum of the signal must be estimated from only the N samples available during a single bit interval, and it is not difficult to show that the sample skewness coefficient of a data sample of length N cannot be larger than $\sqrt{N}$. In fact, the only sequences that actually attain the maximum sample skewness are of the form:

$$u(k) = \sqrt{N}\left(\delta_N(k) - \frac{1}{N}\right), \tag{1}$$

where $\{\delta_N(k)\}_{k=0}^{N-1}$ is any circular shift of a unit impulse sequence of length N. Since we have the luxury of using pseudo-random rather than truly random sequences in our modulation scheme, we will always choose the sequences $\{u(k)\}$ to be of form (1).

Finally, for the purposes of this study, we always used an averaging factor of $c = 0.5$, and we employed filters $\{h_N(k)\}$ that were scaled versions of a canonical low-pass filter; that is,

$$H(\omega) = \begin{cases} 1 & \text{if } |\omega| \le \pi, \\ 0 & \text{otherwise.} \end{cases}$$

This completely describes the signals used in this study. Henceforth, we will refer to these signals as generalized, phase-coupled FSK (GPCFSK) waveforms and to detectors designed to exploit the HOM structure of such signals as HOM detectors.

4. Performance in AWGN

We begin our analysis of the performance characteristics of bispectral modulation techniques by considering the classical AWGN channel. That is, we assume that the received signal sequence $\{r(n)\}$ takes the form:

$$r(n) = x(n) + w(n),$$

where $\{x(n)\}$ is a GPCFSK signal, and $\{w(n)\}$ is a zero-mean, white Gaussian noise process with variance σ_w^2. As discussed in Section 2, we used the Brillinger-Rosenblatt technique to generate estimates of bispectra as well as estimates of normalization factors that were in turn used to compute bicoherence estimates. Throughout the remainder of this report, we will make frequent reference to the asymptotic distributions of the estimates $|\hat{B}_N(\lambda_1,\lambda_2)|^2$, $|\hat{B}_N(\lambda_4,\lambda_5)|^2$, $|\hat{Z}_N(\lambda_1,\lambda_2)|^2$, and $|\hat{Z}_N(\lambda_4,\lambda_5)|^2$, where (λ_1,λ_2) is the normalized frequency pair in D_3 associated with the bit value $b = 0$, and (λ_4,λ_5) is the pair associated with $b = 1$. If we let

$$\sigma_{B,0}^2 = \mathrm{Var}\{\hat{B}_N(\lambda_1,\lambda_2)\}, \quad \mu_{B,0}^2 = |\mathrm{E}\{\hat{B}_N(\lambda_1,\lambda_2)\}|^2,$$

$$\sigma_{B,1}^2 = \mathrm{Var}\{\hat{B}_N(\lambda_4,\lambda_5)\}, \quad \mu_{B,1}^2 = |\mathrm{E}\{\hat{B}_N(\lambda_4,\lambda_5)\}|^2,$$

$$\sigma_{Z,0}^2 = \mathrm{Var}\{\hat{Z}_N(\lambda_1,\lambda_2)\}, \quad \mu_{Z,0}^2 = |\mathrm{E}\{\hat{Z}_N(\lambda_1,\lambda_2)\}|^2,$$

$$\sigma_{Z,1}^2 = \mathrm{Var}\{\hat{Z}_N(\lambda_4,\lambda_5)\}, \quad \mu_{Z,1}^2 = |\mathrm{E}\{\hat{Z}_N(\lambda_4,\lambda_5)\}|^2,$$

then it follows from the asymptotic distribution theory developed in [2] that the distributions in question can be approximated as follows:

$$|\hat{B}_N(\lambda_1,\lambda_2)|^2 \sim \frac{\sigma_{B,0}^2}{2}\cdot\chi_2^2\left(2\frac{\mu_{B,0}^2}{\sigma_{B,0}^2}\right), \quad |\hat{Z}_N(\lambda_1,\lambda_2)|^2 \sim \sigma_{Z,0}^2\cdot\chi_1^2\left(\frac{\mu_{Z,0}^2}{\sigma_{Z,0}^2}\right),$$

$$|\hat{B}_N(\lambda_4,\lambda_5)|^2 \sim \frac{\sigma_{B,1}^2}{2}\cdot\chi_2^2\left(2\frac{\mu_{B,1}^2}{\sigma_{B,1}^2}\right), \quad |\hat{Z}_N(\lambda_4,\lambda_5)|^2 \sim \sigma_{Z,1}^2\cdot\chi_1^2\left(\frac{\mu_{Z,1}^2}{\sigma_{Z,1}^2}\right).$$

Here, we have used the notation $\chi^2_m(\lambda)$ to indicate a non-central chi-squared distribution with m degrees of freedom and non-centrality parameter λ. If we assume that separable rectangular averaging windows and an averaging parameter of $c = 0.5$ are used in all B-R estimates, then it follows from the results in [2] that,

$$\mu^2_{B,0} \approx \frac{E_b^3}{3 \cdot 2^7} N^{-1/2}, \quad \sigma^2_{B,0} \approx \frac{\sigma_w^6}{2^3 \cdot 3^3} N^{-3/2} \left(\gamma_b + 6N^{1/2}\right)^3,$$

$$\mu^2_{Z,0} \approx \frac{\sigma_w^6}{2^9} N^{-3/2} \left(\gamma_b + 6N^{1/2}\right)^3, \quad \sigma^2_{Z,0} \approx \frac{\sigma_w^6}{2^7 \cdot 3} N^{-2} \left(\gamma_b + 6N^{1/2}\right)^3,$$

$$\mu^2_{B,1} \approx 0, \quad \sigma^2_{B,1} \approx \sigma_w^6, \quad \mu^2_{Z,1} \approx \frac{3^3}{2^6} \sigma_w^6, \quad \sigma^2_{Z,1} \approx \frac{3^2}{2^4} N^{-1/2} \sigma_w^6,$$

where E_b represents the energy transmitted in each bit sequence, σ_w^2 represents the power spectral density (i.e., variance) of the AWGN process, and γ_b represents the signal-to-noise ratio (SNR), given by $\gamma_b = E_b / \sigma_w^2$.

Now consider a bicoherence detector that employs the following decision rule to decide whether $b = 0$ or $b = 1$ has been transmitted:

$$\delta(\{r(n)\}) = \begin{cases} 0 \text{ if } \hat{\beta}_0^2 \geq \hat{\beta}_1^2, \\ 1 \text{ if } \hat{\beta}_0^2 < \hat{\beta}_1^2, \end{cases}$$

where we have adopted the notation:

$$\hat{\beta}_0^2 = \frac{\left|\hat{B}_N(\lambda_1, \lambda_2)\right|^2}{\left|\hat{Z}_N(\lambda_1, \lambda_2)\right|^2}, \quad \hat{\beta}_1^2 = \frac{\left|\hat{B}_N(\lambda_4, \lambda_5)\right|^2}{\left|\hat{Z}_N(\lambda_4, \lambda_5)\right|^2}.$$

Assuming that $b = 0$ is sent, the theoretical probability of error (P_e) for such a detector is given by:

$$\begin{aligned} P_e &= P\left\{\hat{\beta}_0^2 < \hat{\beta}_1^2\right\} \\ &\approx P\left\{\frac{\chi_2^2(\lambda)}{\chi_1^2\left(\frac{3}{4}N^{1/2}\right)} < \frac{\chi_2^2(0)}{\chi_1^2\left(\frac{3}{4}N^{1/2}\right)}\right\}, \quad \left(\lambda = \frac{3^2 \gamma_b^3 N}{2^3\left(\gamma_b + 6N^{1/2}\right)^3}\right) \\ &\approx P\left\{F_{\frac{a}{1+d}, \frac{3}{8}N^{1/2}} < \frac{2}{a} F_{2, \frac{3}{8}N^{1/2}}\right\}, \quad \left(a = 2 + \lambda, \ d = \frac{\lambda}{a}\right), \end{aligned}$$

where the symbol $F_{m,n}$ represents an F distribution with m and n degrees of freedom, and the final expression is meant to be interpreted in accordance with the statement "the probability that a random variable with distribution $F_{k,l}$ is less than a constant times an independent random variable with distribution $F_{m,n}$."

Similarly, a detector based on the bispectrum rather than the bicoherence would have a theoretical

P_e given by:

$$\begin{aligned} P_e &= P\left\{\left|\hat{B}_N(\lambda_1,\lambda_2)\right|^2 < \left|\hat{B}_N(\lambda_4,\lambda_5)\right|^2\right\} \\ &\approx P\left\{\frac{\sigma_{B,0}^2}{2}\chi_2^2\left(2\frac{\mu_{B,0}^2}{\sigma_{B,0}^2}\right) < \frac{\sigma_{B,1}^2}{2}\chi_2^2\left(2\frac{\mu_{B,1}^2}{\sigma_{B,1}^2}\right)\right\} \\ &\approx P\left\{F_{\frac{a}{1+d},2} < \frac{2}{a}\frac{\left(6N^{1/2}\right)^3}{\left(\gamma_b + 6N^{1/2}\right)^3}\right\}. \end{aligned}$$

To get some idea of how this performance compares with the performance of more conventional detectors, we note that if one ignores the phase coupling of the three carriers comprising the signal, the optimal noncoherent detection strategy is to compare the outputs of two envelope detectors matched to the modulation (i.e., spreading) sequence $\{m(k)\}$ and appropriate carrier frequencies. The performance of such a detector (as discussed, for example, in [4]) is given by:

$$P_e^* = \frac{1}{2}e^{-\gamma_b/4},$$

which is identical to the performance of the optimal noncoherent detector for conventional binary FSK signals in AWGN [5]. The theoretical performance of the bicoherence and bispectrum detectors relative to this optimal detector performance is illustrated in Figures 2 and 3 for several values of the parameter N. As one would expect, the optimal detector outperforms both of the HOM detectors regardless of the length of the bit interval, but the performance of the bicoherence detectors clearly improves as N increases.

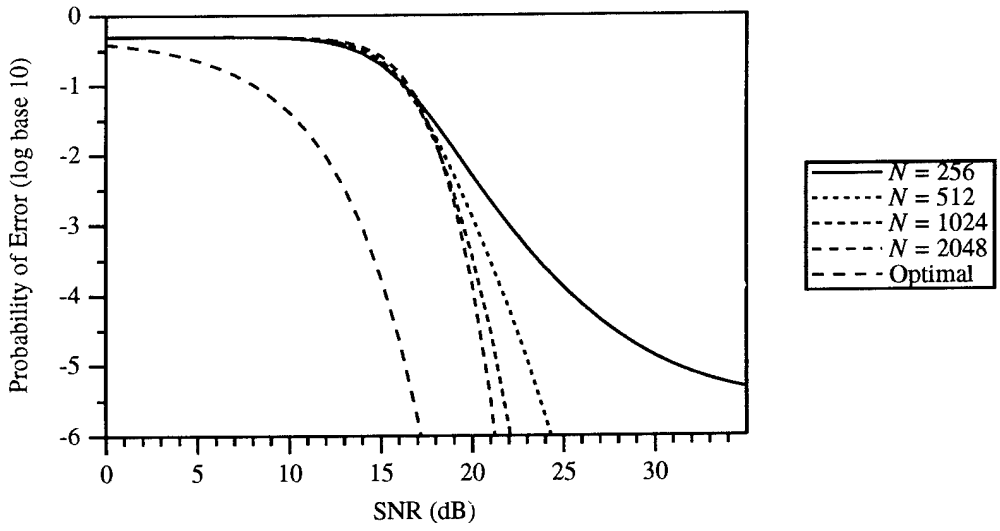

Figure 2. Theoretical Performance of Bicoherence Detector on AWGN Channel

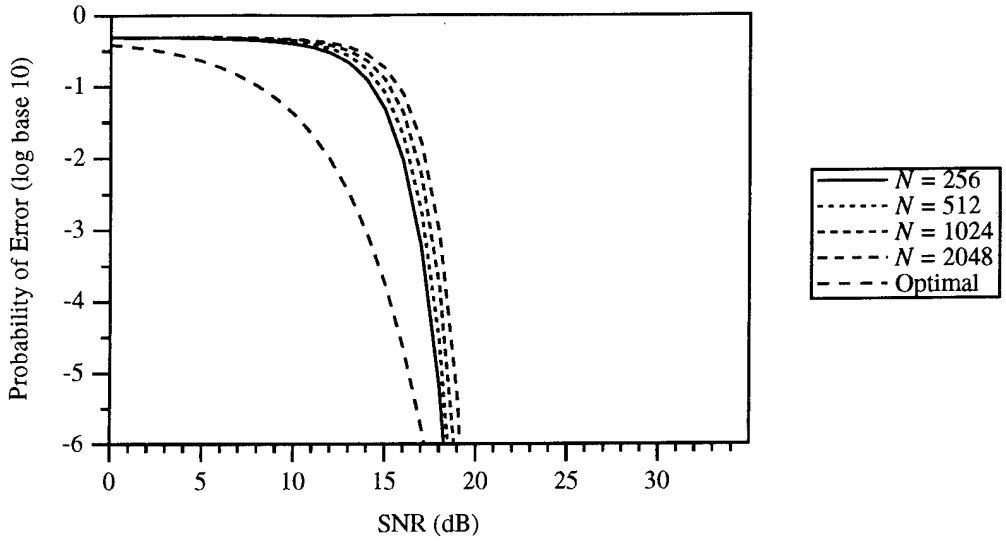

Figure 2. Theoretical Performance of Bispectrum Detector on AWGN Channel

It should be noted that the bispectrum detector significantly outperforms the bicoherence detector at higher SNRs. This is to be expected on AWGN channels, but on channels that exhibit significant, frequency-selective fading, the performance of the bispectrum detector can be expected to deteriorate substantially while the performance of the bicoherence detector should remain relatively stable.

In order to validate our theoretical predictions of the performance of the HOM detectors on an AWGN channel, we performed several simulation studies. The results of the simulations are displayed graphically, relative to the theoretical performance predictions, in Figures 4-11.

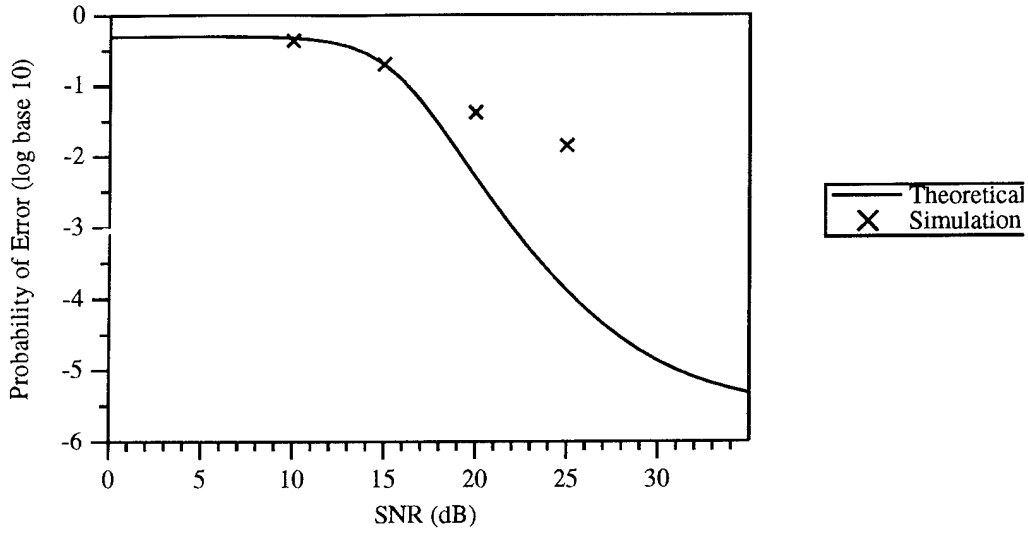

Figure 4. Performance of Bicoherence Detector on AWGN Channel ($N = 256$)

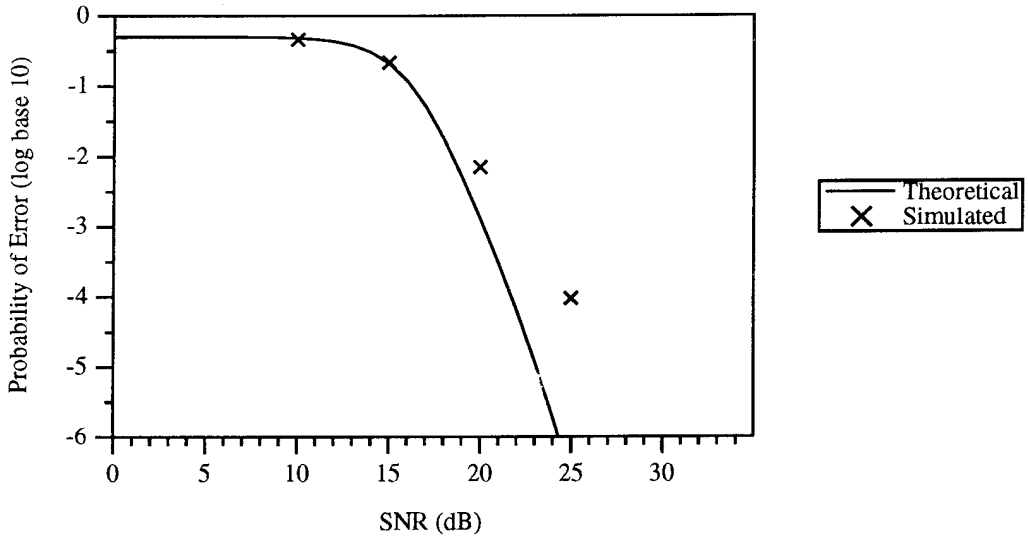

Figure 5. Performance of Bicoherence Detector on AWGN Channel ($N = 512$)

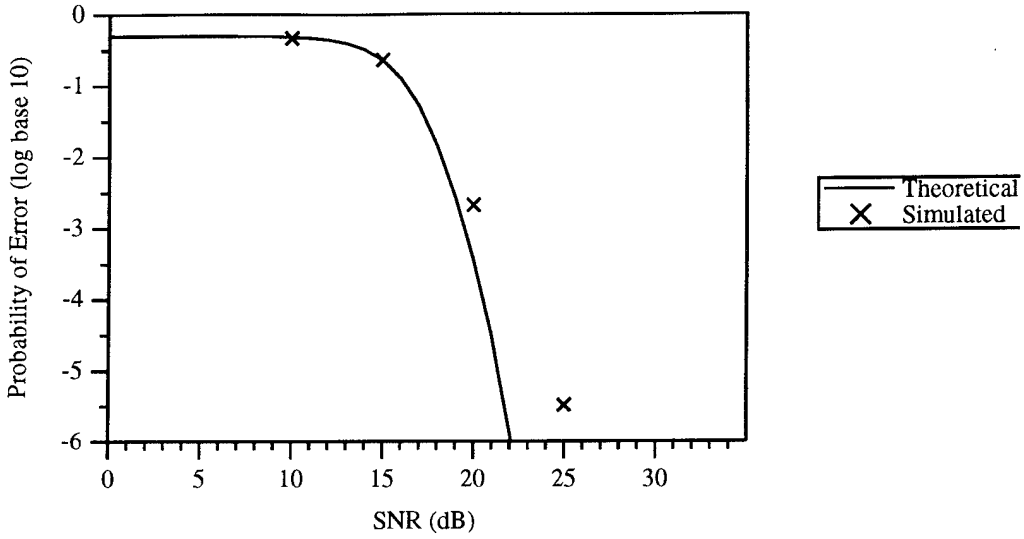

Figure 6. Performance of Bicoherence Detector on AWGN Channel ($N = 1024$)
(The simulated value for P_e at 25 dB is an approximate upper bound. No errors were encountered in 151,200 independent trials.)

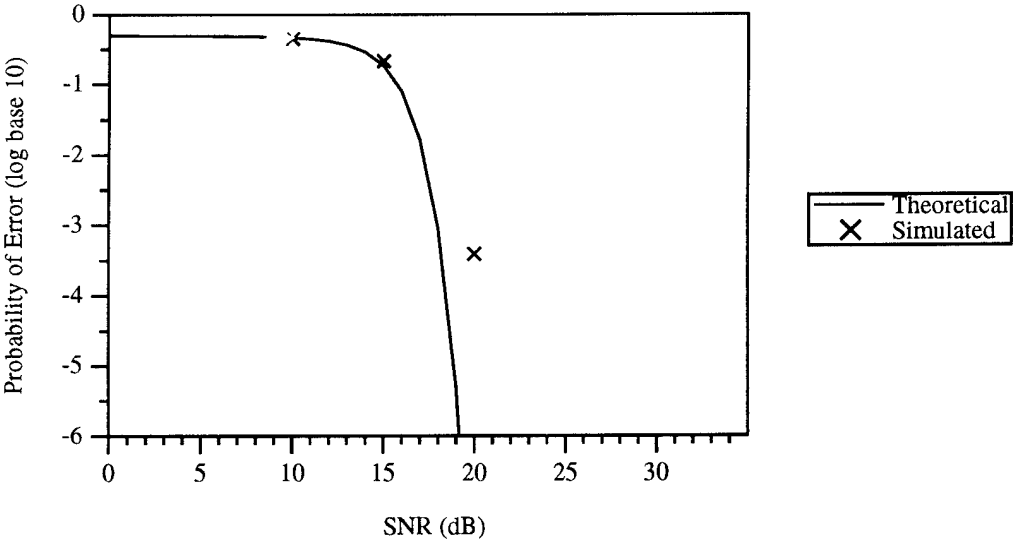

Figure 7. Performance of Bicoherence Detector on AWGN Channel ($N = 2048$)

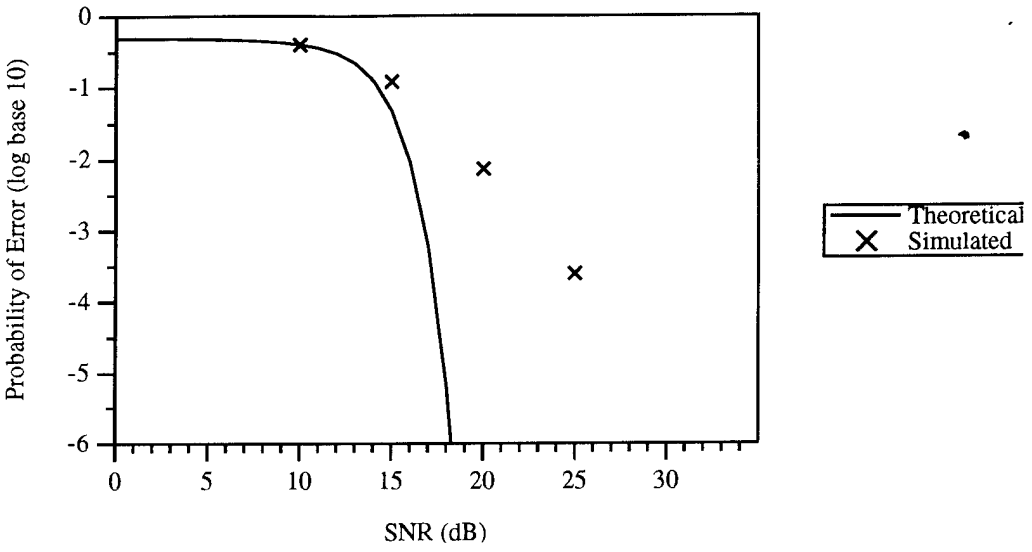

Figure 8. Performance of Bispectrum Detector on AWGN Channel ($N = 256$)

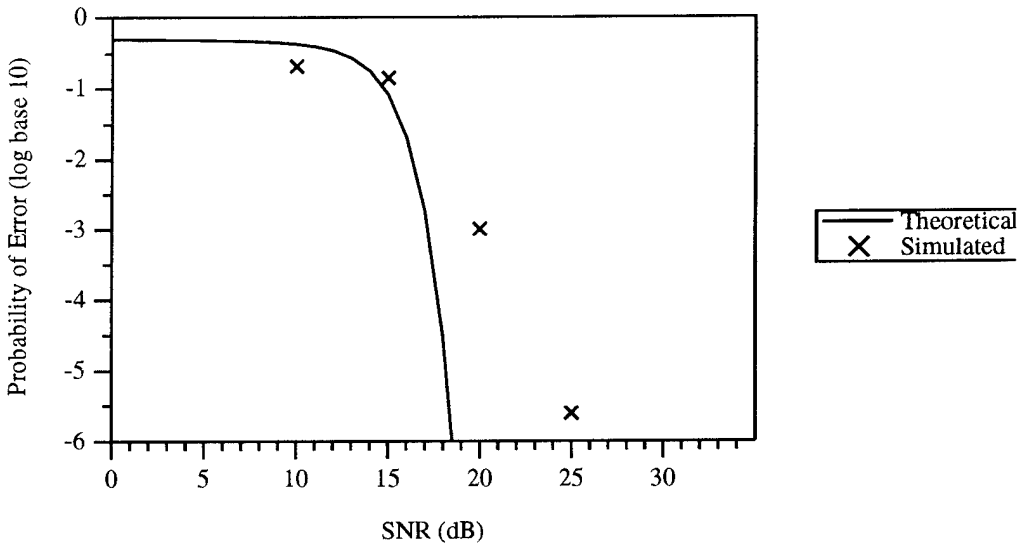

Figure 9. Performance of Bispectrum Detector on AWGN Channel ($N = 512$)

(The value for P_e at 25 dB is an approximate upper bound. No errors were encountered in 202,400 independent trials.)

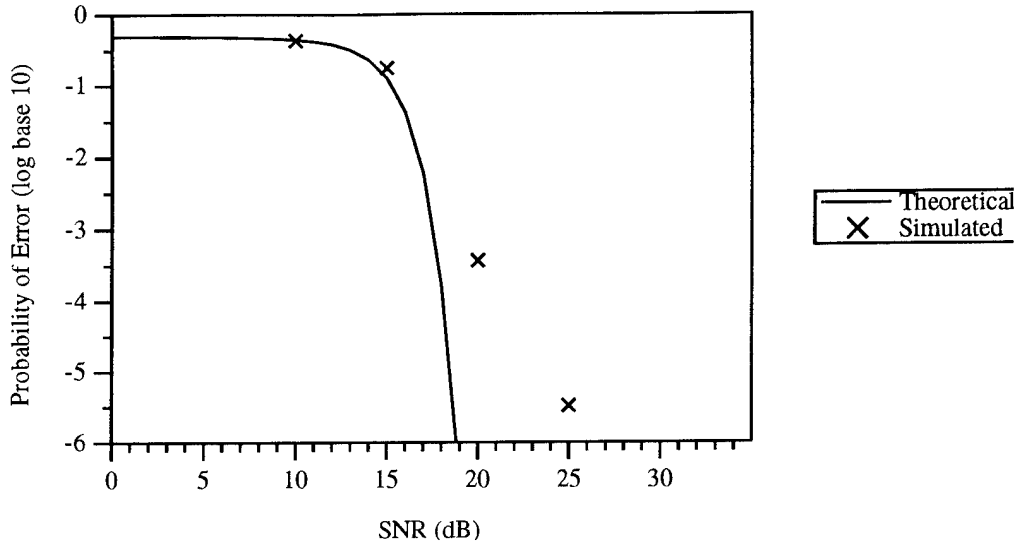

Figure 10. Performance of Bispectrum Detector on AWGN Channels (N = 1024)
(The simulated value for P_e at 25 dB is an approximate upper bound. No errors were encountered in 151,200 independent trials.)

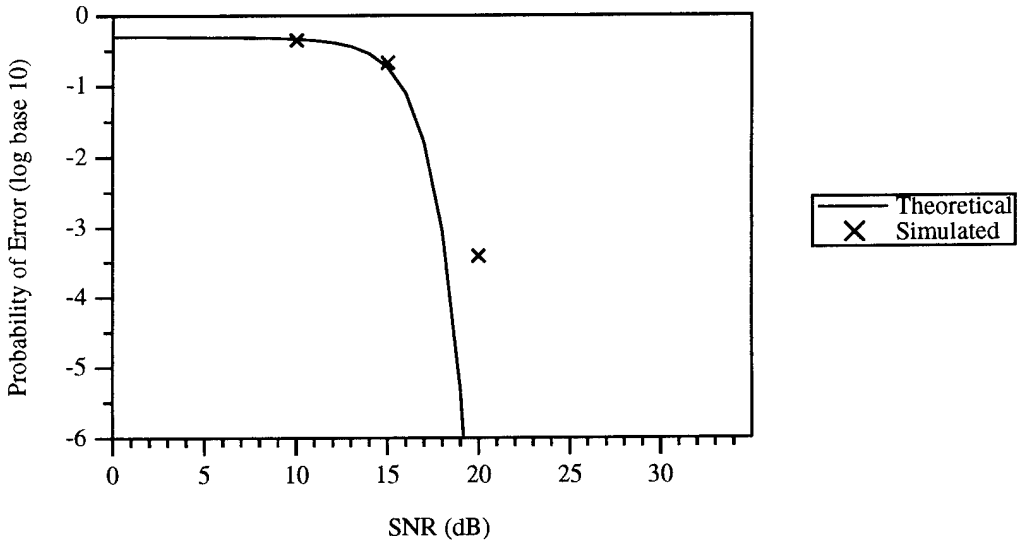

Figure 11. Performance of Bispectrum Detector on AWGN Channel (N = 2048)

As these figures indicate, the correspondence between the theoretical performance results and the simulation results is similar for both the bicoherence and bispectrum detectors. In particular, for bit intervals of length 1024 points or more, the theoretical results are well supported by the

simulations. The fact that larger values of N are required to produce simulation performance that agrees with theoretical predictions is not surprising since the theoretical results are all based on asymptotic distribution theory; that is, the theory is only valid as N goes to infinity.

5. Performance in Partial-Band Jamming

In this section, we consider the performance of bispectral modulation in the presence of partial-band jamming. We restrict attention to bicoherence detection strategies since they are somewhat easier to handle analytically than bispectrum detection schemes, both from a theoretical and simulation standpoint. In any case, preliminary analysis indicates that the performance characteristics of the two different strategies are quite similar.

We now assume that the received signal takes the form:

$$r(n)=x(n)+j(n),$$

where $\{j(n)\}$ is a zero-mean, band-pass interference process with zero bispectrum, variance σ_j^2 and bandwidth equal to $2\pi\alpha$ radians, with $0 < \alpha < 1$. This implies that a fraction α of the total available bandwidth is being jammed during each bit interval, and we assume that the jammer power is distributed randomly throughout the spectrum. That is, in any bit interval, the power spectral density of the jamming process is identically equal to σ_j^2/α on its region of support, where the region of support varies from one bit interval to the next but always occupies exactly $2\pi\alpha$ radians. This is, of course, equivalent to the assumption that the jammer remains fixed and the user randomly varies the locations of the signal carrier frequencies.

Under these assumptions, it is easy to see that the total probability of error is approximately:

$$P_e=(1-\alpha)^3 P_{e0}+3\alpha(1-\alpha)^2 P_{e1}+3\alpha^2(1-\alpha)P_{e2}+\alpha^3 P_{e3},$$

where P_{ek} represents the probability of error given that exactly k components of the signal have been jammed (i.e., a fraction $k/3$ of the signal bandwidth intersects the region of support of the jammer.) Furthermore, using the asymptotic distribution theory developed in the previous section, it can be shown that:

$$P_{ek} \approx P\left\{F_{\frac{a(k)}{1+d(k)},\frac{81}{224}N^{1/2}} < \frac{2}{a(k)} F_{2,\frac{81}{224}N^{1/2}}\right\},$$

where

$$a(k)=2+\lambda(k),\quad d(k)=\frac{\lambda(k)}{a(k)},$$

$$\lambda(k)=\frac{3\gamma_b^k N}{2\left(\gamma_b+\frac{6}{\alpha}N^{1/2}\right)^k},\quad \gamma_b=\frac{E_b}{\sigma_j^2}.$$

Here again, E_b is the energy in the signal during one bit interval, and σ_j^2 is the total jammer power. The worst-case probability of error for the bicoherence detector in partial-band jamming occurs at the value of α that maximizes the expression for total probability of error given above.

Unfortunately, this optimization problem does not admit a closed-form solution, but an approximate value for the worst-case probability of error can be found numerically for each combination of the parameters N and γ_b.

As a comparison, we consider the performance of a noncoherent binary FSK (BFSK) communication system in the presence of partial-band jamming. It can be shown [5] that the probability of error for such a system is given by:

$$P_e = \frac{\alpha}{2} e^{-\alpha\gamma_b/4}.$$

Similarly, it can be shown that the probability of error for such a system is maximized when $\alpha = \alpha^*$, where

$$\alpha^* = \begin{cases} \dfrac{4}{\gamma_b} & \text{if } \gamma_b \geq 4, \\ 1 & \text{if } \gamma_b < 4. \end{cases}$$

Hence, the worst-case probability of error for the BFSK system is given by:

$$P_e^* = \begin{cases} \dfrac{2}{\gamma_b} & \text{if } \gamma_b \geq 4, \\ \dfrac{1}{2} e^{-\gamma_b/4} & \text{if } \gamma_b < 4. \end{cases}$$

To provide a simple comparison of these two systems, we evaluated numerically the approximate worst-case probabilities of error for the bicoherence detector for several different combinations of N and γ_b. The results of this evaluation are compared graphically with the worst-case probabilities of error for the BFSK system in Figure 12.

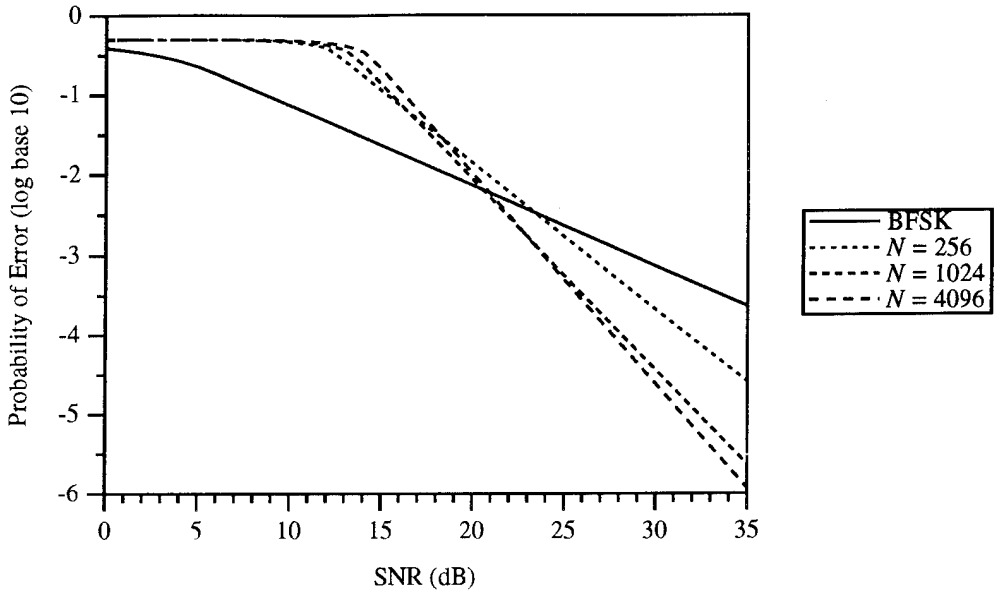

Figure 12. Theoretical Performance of Bicoherence Detector for Worst-Case Partial-Band Jamming

As the figure indicates, the theoretical performance of the bispectral modulation system improves as the value of N increases but stabilizes around $N = 1024$. Furthermore, at higher values of SNR, the bispectral modulation system significantly outperforms the BFSK system in a partial-band jamming environment.

Once again, to validate the theoretical performance predictions, we performed several simulation studies. In this case, we simulated the performance of a bicoherence detector operating on a GPCFSK signal in the presence of a jammer with perfect knowledge of the signal. That is, we assumed that the bandwidth of the jammer was exactly matched to the bandwidth of the signal for all values of N and all three of the signal components were certain to be jammed. Under this scenario, the total probability of error is exactly equal to P_{el3}, which we use as the baseline for comparison with the simulation results. The results of the simulations are presented graphically, relative the theoretical values of P_{el3}, in Figures 13-15.

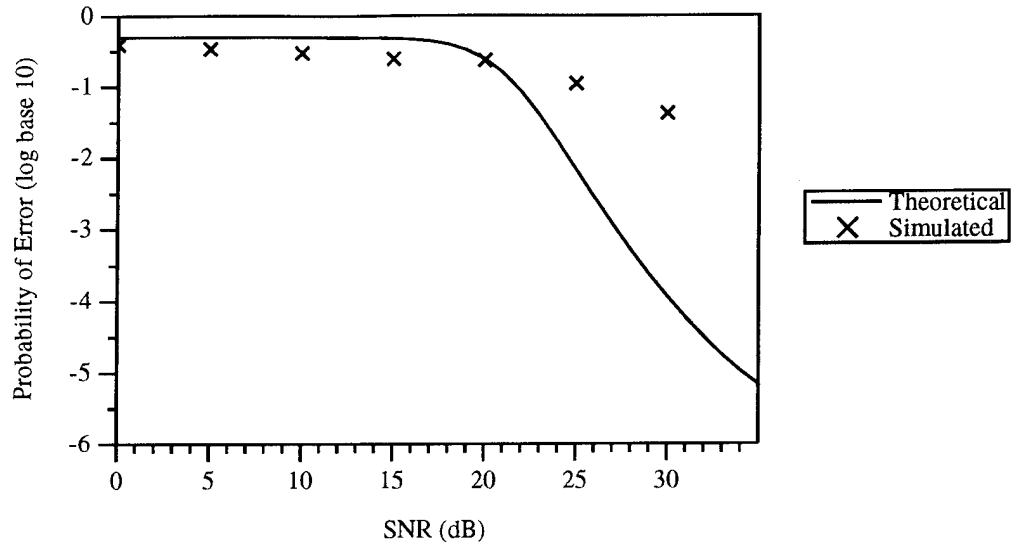

Figure 13. Performance of Bicoherence Detector Against Omniscient Jammer ($N = 256$)

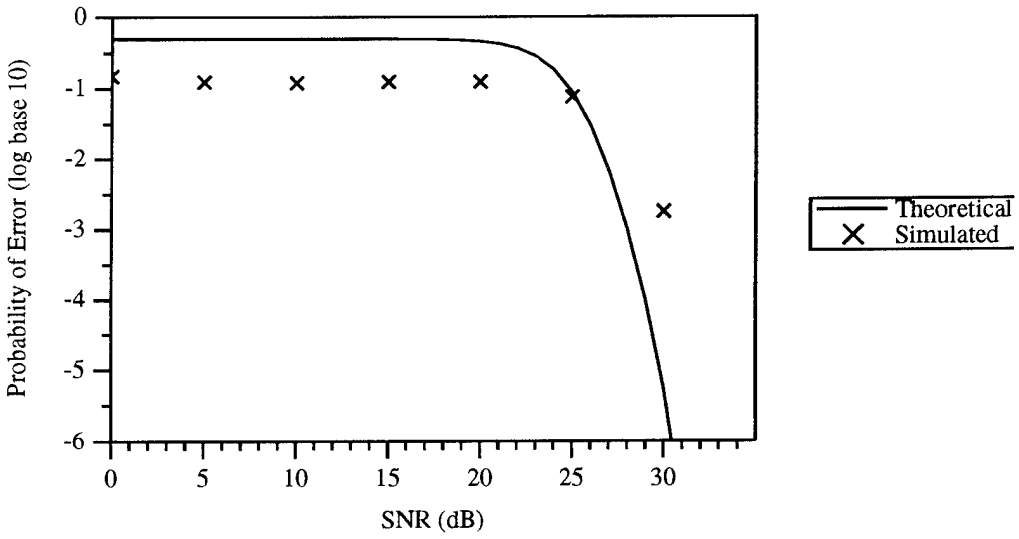

Figure 14. Performance of Bicoherence Detector Against Omniscient Jammer ($N = 1024$)

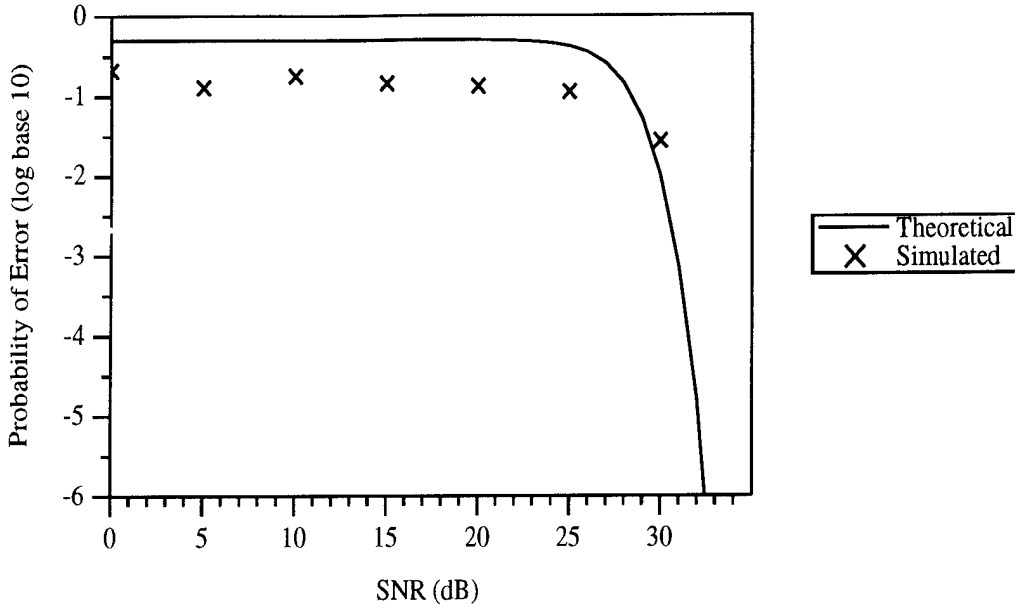

Figure 15. Performance of Bicoherence Detector Against Omniscient Jammer ($N = 4096$)

Again, as the figures indicate, for bit intervals of length 1024 samples or more, the theoretical results are well supported by the simulations. Interestingly, in the low SNR region, where the disparity between the simulations and the theoretical predictions is the greatest, the simulated performance is actually considerably better than predicted. This implies that even for low SNR situations, the theoretical results provide a lower bound that should be useful for performance predictions.

6. Conclusions

In Phase I of this study, we have completed a thorough performance analysis of one possible design for a digital communication system based on bispectral modulation. We have analyzed the performance on both AWGN channels and partial-band jamming channels and compared that performance to the known performance characteristics of more conventional modulation schemes. As expected, the performance of the bispectral modulation technique on the AWGN channel is inferior to the performance that can be achieved with conventional noncoherent schemes, but the performance in the presence of partial-band jamming is significantly better than conventional schemes in the high SNR regimes. This implies that significantly less power is required to maintain a high data rate in a jamming environment when using bispectral modulation than when using conventional modulation such as BFSK. Clearly, this has implications not only for channels subject to intentional jamming, but also for situations where two or more frequency-hopped systems are operating in close proximity to one another, or where two adjacent cells in a cellular network are required to employ some frequency reuse.

Even in a relatively benign AWGN environment, bispectral modulation may offer some advantages over conventional approaches. For example, if covert communication is desired, a GPCFSK system could be employed instead of a simple BFSK system. The system could be used just as a conventional BFSK system in noncovert mode; that is, two modulated frequencies would be

assigned to each of several users, who would transmit on either one frequency or the other depending on the bit value they wished to send. In covert mode, the frequency coupling between a subset of the observable users would be coordinated to transmit an additional data stream that would only be detectable with an HOM detector. The enforced coupling among the chosen subset of users would cause some interference with the remainder of the users but such interference would normally be detectable by the other users, who would simply retransmit. The nonparticipating users would not interfere substantially with the HOM data stream, which would essentially be undetectable by conventional techniques.

Similarly, one could treat a GPCFSK system as a conventional DSSS system in which each user modulates the spreading sequence onto multiple carriers. The optimal receiver for each user would then incorporate envelope detectors matched to the spreading sequence at each of the appropriate frequencies. Naturally, such a detection scheme requires that the detectors acquire and track the phase of the chip sequences in order to give optimal performance, and performance could be substantially degraded if the detectors were not properly synchronized. In contrast, an HOM detector, which could be run in parallel to the conventional detector, requires only relatively crude synchronization in order to maintain stable performance characteristics. In this case, an intelligent combination of the two detection strategies could enhance the overall performance of the system.

It is clear from the results of this study that polyspectral modulation techniques in general, and bispectral modulation in particular, can provide improved performance over conventional modulation strategies in some situations. Considerably more research involving the various modulation techniques available will be required to determine the true extent of the performance advantages and the feasibility of the various alternatives. We believe that our Phase I results strongly suggest that such additional research is warranted.

References

[1] D. W. Pace, "Phase Coupling Detection Techniques," University of Southern California, Ph. D. Dissertation 1992.

[2] D. R. Brillinger and M. Rosenblatt, "Asymptotic Theory of kth Order Spectra," in *Spectral Analysis of Time Series*, B. Harris, Ed. New York: John Wiley and Sons, Inc., 1967.

[3] R. J. Barton, "An Efficient Algorithm for Trispectral Estimation," presented at Twenty-fourth Asilomar Conference on Signals, Systems, & Computers, Pacific Grove, CA, 1990.

[4] H. V. Poor, *An Introduction to Signal Detection and Estimation*, Second ed. New York: Springer-Verlag, 1994.

[5] J. G. Proakis, *Digital Communications*, Second ed. New York: McGraw-Hill, Inc., 1989.